RESEARCH PAPER

Surface functionalization-dependent antioxidant, hemocompatible, and angiogenic responses of Fe_3O_4 nanoparticles

Shaikh Arif Shaikh Iqbal[1,5], S.N. Sowjanya Reddy[2], Qureshi Alfaiz Shaikh Iqbal[3], Jyoti Mayekar[4], Radha S[1], Md. Rageeb Md. Usman[3*]

[1]Department of Physics, University of Mumbai, Maharashtra, India.
[2]Shah and Anchor Kutchhi Engineering College, Mumbai, Maharashtra, India.
[3]Department of Pharmacognosy, Smt. Sharadchandrika Suresh Patil College of Pharmacy, Chopda, Maharashtra, India. Email: mdrageebusman@gmail.com
[4]Department of Physics, Jai Hind College, Mumbai, Maharashtra, India.
[5]Department of Humanities & Applied Sciences, School of Engineering & Technology, AIKTC, New Panvel, India.

***Corresponding author: Dr. Md. Rageeb Md. Usman**
Professor & HOD, Department of Pharmacognosy, Smt. Sharadchandrika Suresh Patil College of Pharmacy, Chopda, Maharashtra, India

ABSTRACT

Surface modification of magnetic nanoparticles is a widely employed strategy to improve their biological performance and expand their applicability in biomedical systems. In the present study, the biological responses of uncoated Fe_3O_4 nanoparticles (A1), polyethylene glycol-coated Fe_3O_4 nanoparticles (A2), and citric-acid-coated Fe_3O_4 nanoparticles (A3) were investigated through antioxidant, hemocompatibility, and angiogenic evaluations. Antioxidant activity was assessed using the DPPH free radical scavenging assay, while hemocompatibility was examined through erythrocyte membrane stabilization studies. Angiogenic behaviour and vascular compatibility were evaluated using the Hen's Egg Test-Chorioallantoic Membrane (HET-CAM) assay coupled with Fiji/ImageJ-based quantitative vascular analysis.

All nanoparticle formulations exhibited concentration-dependent antioxidant and membrane stabilization activities. Among the investigated samples, A1 demonstrated the highest antioxidant activity, achieving 63.68% DPPH radical scavenging at the maximum tested concentration. In contrast, surface-functionalized nanoparticles showed enhanced membrane stabilization behaviour, with A2 exhibiting the highest membrane stabilization activity (77.19%), followed by A3 (63.52%). Qualitative HET-CAM observations revealed vascular irritation, hemorrhage, and coagulation effects in A1, whereas coated nanoparticles displayed improved vascular compatibility with minimal adverse effects. Quantitative vascular analysis indicated progressive angiogenic development in all samples. Notably, A3 exhibited the better angiogenic response, with vessel area increasing from 14.57% to 47.86% and branch count increasing from 74 to 236 during the 72 h incubation period.

The findings demonstrate that surface modification significantly influences the biological behaviour of Fe_3O_4 nanoparticles. While uncoated nanoparticles exhibited superior antioxidant activity, PEGylation improved hemocompatibility, and citric-acid functionalization promoted enhanced angiogenic response and vascular compatibility. These results highlight the importance of surface engineering in tailoring Fe_3O_4 nanoparticles for potential drug delivery and biomedical applications.

Keywords: Fe_3O_4 nanoparticles, surface functionalization, PEGylation, citric acid coating, antioxidant activity, hemocompatibility, angiogenesis, HET-CAM assay.

How to cite this article: Iqbal SAS, Reddy SNS, Iqbal QAS, Mayekar J, Radha S, Usman MRM. Surface functionalization-dependent antioxidant, hemocompatible, and angiogenic responses of Fe_3O_4 nanoparticles. Int J Drug Deliv Technol. 2026;16(59s): 335-343. DOI: 10.25258/ijddt.16.59s.32

Source of support: Nil

Conflict of interest: None

1. INTRODUCTION

Magnetic nanoparticles have attracted considerable attention owing to their unique physicochemical and magnetic properties, which make them suitable for a wide range of biomedical applications including targeted drug delivery, magnetic resonance imaging, hyperthermia therapy, biosensing, and tissue engineering[1,2,3]. Among the various magnetic nanomaterials, magnetite (Fe_3O_4) nanoparticles are particularly attractive because of their biocompatibility, chemical stability, superparamagnetic behaviour, and ease of synthesis[4,5]. Furthermore, their high surface-area-to-volume ratio facilitates interactions with biological molecules and cellular systems, thereby enhancing their applicability in biomedical and pharmaceutical formulations[6].

Despite these advantages, the biological performance of Fe_3O_4 nanoparticles is strongly

dependent on their surface characteristics. Bare nanoparticles often exhibit a tendency to aggregate in aqueous and physiological environments because of magnetic dipole interactions and high surface energy, which may adversely affect their colloidal stability and biological response[7,8]. Surface functionalization has therefore emerged as an effective strategy to improve nanoparticle stability, dispersibility, and biocompatibility[9]. Among the various coating materials, polyethylene glycol (PEG) is widely employed because it enhances hydrophilicity, reduces nonspecific protein adsorption, and prolongs circulation time in biological systems[10,11]. Similarly, citric acid is frequently used as a stabilizing agent due to the presence of carboxyl groups that provide electrostatic repulsion and improve aqueous dispersibility and colloidal stability[12,13].

For biomedical applications, it is essential to evaluate the interaction of nanoparticles with blood components and biological membranes. Hemocompatibility studies provide valuable information regarding the safety of nanomaterials intended for systemic administration. Membrane stabilization assays are commonly used to assess the ability of materials to protect erythrocyte membranes against osmotic or chemically induced damage and are often considered indicators of anti-inflammatory and membrane-protective potential[14,15]. Nanoparticles exhibiting favourable membrane stabilization characteristics are expected to demonstrate improved compatibility with biological systems.

Another important aspect in the biomedical evaluation of nanoparticles is their antioxidant activity. Oxidative stress generated by excessive reactive oxygen species (ROS) has been implicated in numerous pathological conditions, including inflammation, cardiovascular disorders, diabetes, and cancer[16]. Consequently, materials capable of scavenging free radicals may contribute to the reduction of oxidative damage and improvement of cellular health. The DPPH radical scavenging assay is one of the most widely used methods for evaluating the antioxidant potential of nanomaterials because of its simplicity, sensitivity, and reproducibility[17,18].

In addition to antioxidant and hemocompatibility assessments, the evaluation of vascular compatibility and angiogenic behaviour has become increasingly important for nanomaterials intended for biomedical and drug delivery applications. Angiogenesis, the process of new blood vessel formation from existing vasculature, plays a crucial role in tissue regeneration, wound healing, and therapeutic recovery[19]. Depending on their physicochemical properties and surface chemistry, nanoparticles may either promote vascular development or induce vascular irritation and damage. Therefore, understanding nanoparticle-induced vascular responses is essential for predicting their biological safety and therapeutic applicability.

The Hen's Egg Test–Chorioallantoic Membrane (HET-CAM) assay is widely recognized as a simple, rapid, and cost-effective model for investigating vascular irritation and angiogenic responses[20]. The assay enables direct visualization of vascular morphology and allows the assessment of parameters such as hemorrhage, vascular lysis, coagulation, vessel density, and vascular branching. Combined with digital image analysis techniques, HET-CAM provides valuable qualitative and semi-quantitative information regarding nanoparticle–vascular interactions[21].

Although numerous studies have reported the synthesis and physicochemical characterization of Fe_3O_4 nanoparticles, comprehensive evaluation of how surface modification influences antioxidant activity, hemocompatibility, and angiogenic behaviour remains limited[22]. In particular, comparative investigations involving uncoated and surface-functionalized Fe_3O_4 nanoparticles can provide valuable insights into the role of surface chemistry in determining biological performance. Detailed physicochemical characterization of the synthesized nanoparticle formulations has been reported separately[23]. However, their comparative biological responses remain insufficiently explored. Therefore, the present study investigates the biological responses of uncoated Fe_3O_4 nanoparticles (A1), PEG-coated Fe_3O_4 nanoparticles (A2), and citric-acid-coated Fe_3O_4 nanoparticles (A3). Antioxidant activity was evaluated using the DPPH radical scavenging assay, while hemocompatibility was assessed through membrane stabilization studies. Furthermore, angiogenic response and vascular compatibility were examined using the HET-CAM assay coupled with Fiji/ImageJ-based vascular analysis. The findings provide insight into the influence of surface modification on the biological behaviour of Fe_3O_4 nanoparticles and their potential utilization in future biomedical and drug-delivery-related applications.

2. MATERIALS AND METHODS

2.1 Materials

Ferric chloride hexahydrate ($FeCl_3 \cdot 6H_2O$), ferrous chloride tetrahydrate ($FeCl_2 \cdot 4H_2O$), polyethylene glycol (PEG-6000), citric acid, aqueous ammonia solution, ethanol, and 2,2-diphenyl-1-picrylhydrazyl (DPPH) were procured from standard commercial sources and used without further purification. Deionized water was used

throughout the synthesis, washing, and biological evaluation procedures. Polyethylene glycol and citric acid were utilized as surface-functionalizing agents for Fe_3O_4 nanoparticles. Ascorbic acid and aspirin were employed as reference standards for antioxidant and membrane stabilization studies, respectively. Fertilized embryonated hen eggs used for angiogenesis evaluation were obtained from a local hatchery and incubated under controlled laboratory conditions prior to experimentation.

2.2 Synthesis of Fe_3O_4 Nanoparticles

2.2.1 Preparation of Uncoated Fe_3O_4 Nanoparticles (A1)

Magnetite nanoparticles were synthesized by a chemical co-precipitation method. Briefly, $FeCl_3 \cdot 6H_2O$ (10.812 g) and $FeCl_2 \cdot 4H_2O$ (2.535 g) were dissolved in 200 mL of deionized water under continuous magnetic stirring while maintaining a Fe^{3+}:Fe^{2+} molar ratio of 2:1. The reaction mixture was heated to 65°C, followed by the gradual addition of aqueous ammonia solution until the pH reached 12-14. The appearance of a black precipitate indicated the formation of Fe_3O_4 nanoparticles. The nanoparticles were collected by magnetic decantation and washed repeatedly with deionized water and ethanol until neutral pH was achieved. The purified nanoparticles were dried at 50 °C for 10 h and designated as A1.

2.2.2 Preparation of PEG-Coated Fe_3O_4 Nanoparticles (A2)

PEG-functionalized Fe_3O_4 nanoparticles were synthesized using the same co-precipitation procedure. Prior to alkaline precipitation, 0.5 g of PEG-6000 was dissolved in the precursor solution containing the iron salts. The subsequent precipitation, washing, and drying steps were identical to those employed for A1. The resulting PEG-coated nanoparticles were designated as A2.

2.2.3 Preparation of Citric-Acid-Coated Fe_3O_4 Nanoparticles (A3)

Citric-acid-coated Fe_3O_4 nanoparticles were prepared through a modified co-precipitation approach. During nanoparticle formation, 0.5 g of citric acid was introduced into the reaction mixture simultaneously with the ammonia solution under continuous stirring. The pH was maintained between 12 to 14 throughout the precipitation process. After completion of the reaction, the nanoparticles were magnetically separated, thoroughly washed with deionized water and ethanol, and dried at 50 °C for 10 h. The obtained sample was labelled as A3.

2.3 Nanoparticle Formulations

Three Fe_3O_4 nanoparticle formulations were investigated in the present study, namely uncoated Fe_3O_4 nanoparticles(A1), PEG-coated Fe_3O_4 nanoparticles(A2), and citric-acid-coated Fe_3O_4 nanoparticles(A3). Detailed physicochemical characterization of these formulations, including structural, morphological, surface, colloidal, and magnetic analyses, has been reported in our previous work available as a preprint[23]. The characterization confirmed the successful formation of Fe_3O_4 nanoparticles and the effectiveness of the respective surface functionalization strategies. Therefore, the present study focuses exclusively on the comparative biological evaluation of the nanoparticle formulations through antioxidant, hemocompatibility, and angiogenesis assays.

Table 1: Physicochemical properties of synthesized Fe_3O_4 nanoparticles

Sample	Coating	Crystallite Size (nm)	Hydrodynamic Diameter (nm)	Zeta Potential (mV)	Ms (emu/g)
A1	None	26	99	-6.8	71.1
A2	PEG 6000	19	91	-18.4	57.7
A3	Citric Acid	18	97	-31.4	64.8

The physicochemical characteristics of the nanoparticle formulations are summarized in Table1. Surface functionalization resulted in a reduction in crystallite size and a marked increase in negative surface charge, indicating improved colloidal stability. The citric-acid-coated nanoparticles (A3) exhibited the highest negative zeta potential (-31.5 mV). These differences are expected to influence nanoparticle-biological interactions and may contribute to variations in antioxidant, hemocompatibility, and angiogenic responses observed in the present study.

2.4 DPPH Radical Scavenging Assay

The antioxidant activity of the synthesized nanoparticles was evaluated using the DPPH free radical scavenging method. Different concentrations of nanoparticle suspensions were prepared and mixed with 0.1% methanolic DPPH solution. Briefly, 1 mL of nanoparticle suspension was added to 1.5 mL of DPPH solution and incubated in the dark for 30 min at room temperature. Following incubation, the absorbance was measured at 517 nm using a UV-Visible spectrophotometer. Ascorbic acid was used as the reference antioxidant standard. The percentage radical scavenging activity was calculated according to;

$$DPPH\ scavenging\ activity(\%) = \frac{A_{control} - A_{sample}}{A_{control}} x$$

where $A_{control}$ and A_{sample} represent the absorbance values of the control and samples

respectively. All measurements were performed in triplicates.

2.5 Membrane Stabilization Assay

The membrane stabilization potential of the synthesized nanoparticles was evaluated using a red blood cell (RBC) membrane stabilization assay. Fresh blood samples were centrifuged at 3000 rpm for 10 min, and the packed erythrocytes were washed three times with normal saline solution. A 10% (v/v) RBC suspension was subsequently prepared. For the assay, 1 mL of nanoparticle suspension was mixed with 1 mL of RBC suspension. Aspirin served as the reference standard, while normal saline was used as the control. The mixtures were incubated at 56 °C for 30 min and then centrifuged at 2500 rpm for 5 min. The absorbance of the supernatant was recorded at 560 nm.

Percentage hemolysis and membrane stabilization were calculated using the following equations:

$$Hemolysis(\%) = \frac{OD_{test}}{OD_{control}} \times 100$$

$$Membrane\ Stabilization(\%) = \left[1 - \frac{OD_{test}}{OD_{control}}\right] \times 100$$

where OD_{test} is optical density or the test sample's absorbance and $OD_{control}$ is optical density or absorbance of the negative control. All experiments were conducted in triplicate.

2.6 HET-CAM Angiogenesis Assay

The angiogenic response and vascular compatibility of the synthesized nanoparticles were investigated using the Hen's Egg Test-Chorioallantoic Membrane (HET-CAM) assay. Fertilized embryonated hen eggs were incubated under controlled temperature and humidity conditions. After incubation, a small opening was carefully created in the eggshell to expose the chorioallantoic membrane (CAM) without disturbing the developing embryo.

An untreated CAM served as the control group, while nanoparticle formulations A1 (uncoated Fe_3O_4), A2 (PEG-coated Fe_3O_4), and A3 (citric-acid-coated Fe_3O_4) were applied onto the CAM surface under sterile conditions. Vascular responses were monitored over a period of 72 h, and representative images were recorded at 0, 24, 48, and 72 h. Qualitative observations including hemorrhage, vascular lysis, coagulation, embryo viability, and vascular development were documented to evaluate angiogenic potential and vascular compatibility. Comparisons between the treated groups and the untreated control were used to assess nanoparticle-induced vascular responses and angiogenic activity.

2.7 Fiji/ImageJ-Based Vascular Analysis

To obtain quantitative information regarding angiogenic activity, CAM images acquired at different incubation intervals were analysed using Fiji/ImageJ software. The images were converted to grayscale and subjected to threshold-based segmentation to isolate vascular structures from the background. Binary images were generated and used for vascular quantification. The percentage vessel area was determined from the segmented vascular network, while vascular branching was assessed by counting the number of vessel branches within the selected region of interest. Measurements obtained at different time intervals were used to compare the angiogenic responses of the three nanoparticle formulations.

2.8 Statistical Analysis

All DPPH radical scavenging and membrane stabilization experiments were performed in triplicate, and the results are expressed as mean ± standard deviation (SD). Statistical analysis was carried out using Origin software. One-way analysis of variance (ANOVA) was employed to evaluate differences among the experimental groups, and differences were considered statistically significant at $p < 0.05$.

For the HET-CAM assay, qualitative observations together with image-based quantitative measurements of vessel area percentage and branch count were used to assess angiogenic responses. Owing to the exploratory nature of the CAM imaging study, the angiogenesis results are presented descriptively and comparatively among the nanoparticle formulations.

3. RESULTS AND DISCUSSION

3.1 Antioxidant Activity

The antioxidant potential of uncoated and surface-functionalized Fe_3O_4 nanoparticles was evaluated using the DPPH free radical scavenging assay over a concentration range of 0.01-0.4 μM mL^{-1}. As shown in Fig.1, all nanoparticle formulations exhibited concentration-dependent radical scavenging activity, indicating their ability to neutralize DPPH free radicals. The standard antioxidant, ascorbic acid, demonstrated the highest activity, reaching 89.64% inhibition at 0.4 μM mL^{-1} with an IC_{50} value of 0.07 μM mL^{-1}. Among the nanoparticle formulations, the uncoated Fe_3O_4 sample (A1) exhibited the strongest antioxidant activity, increasing from 11.92% inhibition at 0.01 μM mL^{-1} to 63.73% at 0.4 μM mL^{-1}. The PEG-coated nanoparticles (A2) displayed comparatively lower scavenging activity, achieving 54.40% inhibition at the highest concentration, whereas the citric acid-coated nanoparticles (A3) reached 50.26% inhibition. The calculated IC_{50} values were 0.19, 0.30, and 0.39 μM mL^{-1} for A1, A2, and A3, respectively, confirming the superior radical

scavenging efficiency of the uncoated nanoparticles.

The enhanced antioxidant activity observed for A1 may be attributed to the greater accessibility of surface iron ions capable of participating in electron-transfer processes involved in DPPH radical reduction. Surface coating with PEG or citric acid partially shields the nanoparticle surface, thereby reducing direct interaction between the active iron oxide surface and free radicals. Although functionalization slightly reduced antioxidant performance, both coated formulations retained substantial radical scavenging ability, suggesting that surface modification does not completely inhibit the intrinsic antioxidant characteristics of Fe_3O_4 nanoparticles.

Overall, the antioxidant activity followed the order: Ascorbic acid > A1 > A2 > A3.

These findings demonstrate that surface chemistry significantly influences the free radical scavenging behaviour of Fe_3O_4 nanoparticles and should be carefully considered when designing magnetic nanomaterials for biomedical applications involving oxidative stress modulation.

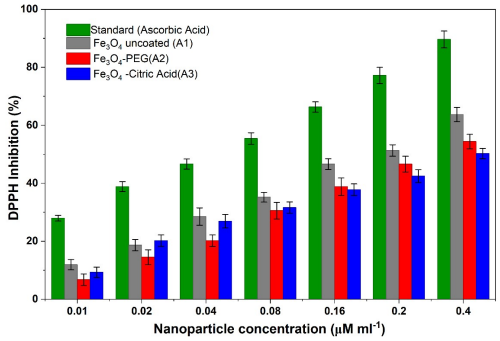

Fig.1: DPPH radical scavenging activity of A1 (uncoated Fe_3O_4), A2 (PEG-coated Fe_3O_4), A3 (citric-acid-coated Fe_3O_4), and ascorbic acid at different concentrations.

3.2 Hemocompatibility Assessment by Membrane Stabilization Assay

The hemocompatibility of the synthesized Fe_3O_4 nanoparticles was evaluated using a red blood cell (RBC) membrane stabilization assay. This method is based on the ability of the test materials to protect erythrocyte membranes against heat-induced hemolysis, which serves as an indicator of membrane integrity and blood compatibility. The percentage membrane stabilization values obtained for the nanoparticle formulations are presented in Fig. 2.

All nanoparticle formulations exhibited concentration-dependent membrane stabilization activity within the investigated concentration range (0.01-0.4 μM mL^{-1}). The standard drug aspirin showed the highest protective effect, increasing from 16.26% stabilization at 0.01 μM mL^{-1} to 87.80% at 0.4 μM mL^{-1}. Among the nanoparticle samples, PEG-coated Fe_3O_4 nanoparticles (A2) demonstrated the strongest membrane protective effect, reaching 77.24% stabilization at the highest concentration. The uncoated Fe_3O_4 nanoparticles (A1) and citric acid-coated Fe_3O_4 nanoparticles (A3) exhibited maximum stabilization values of 65.04% and 63.41%, respectively.

At lower concentrations (0.01-0.04 μM mL^{-1}), all samples displayed relatively modest membrane stabilization activity. However, a pronounced increase was observed with increasing concentration, indicating enhanced interaction between the nanoparticles and erythrocyte membranes. The superior performance of A2 suggests that PEG functionalization improves the interaction of Fe_3O_4 nanoparticles with biological membranes while minimizing membrane disruption. PEG molecules are known to increase hydrophilicity and steric stabilization, thereby reducing direct nanoparticle-membrane damage and improving overall hemocompatibility. The uncoated Fe_3O_4 nanoparticles exhibited moderate membrane protection. Although bare nanoparticles possess active surface sites that may interact with membrane phospholipids, the absence of a protective surface coating may increase the possibility of direct membrane contact, resulting in comparatively lower stabilization efficiency. The citric acid-coated nanoparticles also demonstrated substantial membrane protection; however, their performance remained slightly lower than that of PEG-coated nanoparticles at higher concentrations. The observed hemocompatibility trend is consistent with the zeta potential measurements obtained during physicochemical characterization. The more negative surface charge of the coated nanoparticles, particularly A2 and A3, contributes to improved colloidal stability and reduced aggregation under physiological conditions, thereby promoting favorable interactions with erythrocyte membranes. Furthermore, the lower coercivity and improved dispersion characteristics of the coated formulations may contribute to enhanced biological compatibility.

Overall, membrane stabilization activity followed the order: Aspirin > A2 > A1 ≈ A3.

These findings indicate that surface functionalization significantly improves the blood compatibility of Fe_3O_4 nanoparticles, with PEG coating providing the most effective protection against erythrocyte membrane damage. The results suggest that PEG-functionalized Fe_3O_4 nanoparticles may be more suitable for biomedical applications involving direct contact with blood and vascular tissues.

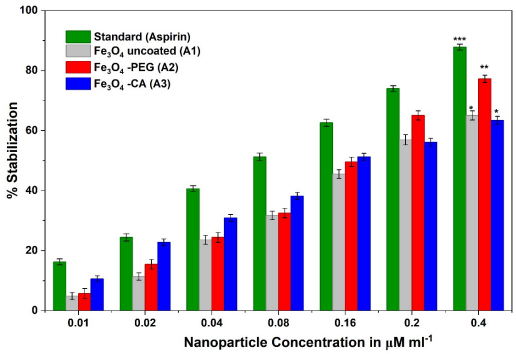

Fig. 2: Concentration-dependent membrane stabilization activity of A1, A2, and A3 Fe_3O_4 nanoparticles compared with aspirin.

3.3 HET-CAM Angiogenic Evaluation

The angiogenic potential and vascular compatibility of the synthesized Fe_3O_4 nanoparticle formulations were investigated using the Hen's Egg Test-Chorioallantoic Membrane (HET-CAM) assay. The CAM model provides a highly vascularized environment for evaluating nanoparticle-induced vascular responses, including hemorrhage, vascular lysis, coagulation, embryo viability, and blood vessel development. Representative CAM images of the untreated control and nanoparticle-treated groups recorded after 72 h of incubation are presented in Fig. 3, while the qualitative observations are summarized in Table 2.

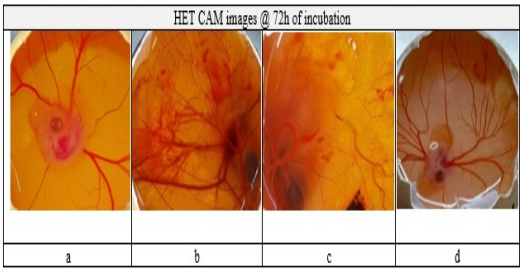

Fig. 3: Representative HET-CAM images after 72 h incubation arranged as:
(a) Control (b) A1 (c) A2 (d) A3

Table 2. Qualitative HET-CAM observations (Control, A1, A2, A3)

Observation	**Control**	**A1**	**A2**	**A3**
Embryo viability	Yes	Yes	Yes	Yes
Hemorrhage	No	Yes	No	No
Vascular lysis	No	Yes	No	No
Coagulation	No	Yes	Slight	No
Angiogenic response	Normal	Moderate	Enhanced	Strongly Enhanced

The control CAM exhibited a normal vascular architecture characterized by well-organized blood vessels radiating from the embryo without signs of vascular damage or irritation. Embryo viability was maintained throughout the observation period, confirming normal developmental progression under the experimental conditions.

In contrast, treatment with uncoated Fe_3O_4 nanoparticles (A1) produced noticeable adverse effects on the CAM vasculature. The treated CAM showed visible hemorrhage, vascular lysis, and coagulation, accompanied by disruption of the vascular organization around the treatment region. The laboratory observations further indicated that the developing embryo was adversely affected during the later stages of incubation, suggesting reduced vascular compatibility of the uncoated nanoparticles. These findings imply that direct exposure of the Fe_3O_4 surface may induce vascular irritation and compromise the integrity of developing blood vessels.

A markedly different response was observed for PEG-coated Fe_3O_4 nanoparticles (A2). No evidence of hemorrhage or vascular lysis was detected throughout the experimental period, and embryo viability was preserved up to 72 h. Although slight coagulation effects were noted during intermediate incubation stages, the vascular network remained intact and continued to develop around the treatment area. The CAM images revealed progressive vessel formation and improved vascular organization compared with A1, indicating enhanced vascular compatibility following PEG functionalization.

Among all formulations, citric-acid-coated Fe_3O_4 nanoparticles (A3) exhibited the most favourable angiogenic profile. No hemorrhage, vascular lysis, or coagulation was observed, and embryo viability was maintained throughout the study period. The CAM displayed a dense, highly organized vascular network with extensive vessel growth surrounding the treatment region. Visual examination suggested enhanced neovascularization and increased vessel branching relative to both the control and the other nanoparticle formulations. These observations indicate excellent vascular compatibility and a pronounced pro-angiogenic effect associated with citric acid surface functionalization.

The improved vascular response observed for A2 and A3 may be attributed to the beneficial effects of surface modification on nanoparticle-biological

interactions. Surface coatings improve colloidal stability and reduce direct contact between the magnetic core and vascular tissues, thereby minimizing vascular irritation. In particular, the highly negative surface charge and larger specific surface area of A3 may facilitate more favourable interactions with the CAM microenvironment, supporting blood vessel formation while preserving vascular integrity.

Overall, the qualitative HET-CAM observations demonstrate that surface functionalization significantly influences the biological response of Fe_3O_4 nanoparticles. While uncoated nanoparticles induced signs of vascular irritation and damage, PEG-coated and citric-acid-coated nanoparticles exhibited superior vascular compatibility and promoted blood vessel development. Among the investigated formulations, A3 displayed the strongest angiogenic response, followed by A2, whereas A1 showed comparatively lower vascular compatibility and angiogenic potential.

3.4 Quantitative Analysis of Angiogenesis

To substantiate the qualitative HET-CAM observations, quantitative image analysis was performed using Fiji/ImageJ software. The vascular networks present in the CAM images were evaluated in terms of vessel area percentage and branch count, which are widely used indicators of angiogenic activity. The results are presented in Fig. 4 and Fig. 5.

3.4.1 Vessel Area Analysis

The vessel area percentage increased with incubation time for all nanoparticle formulations, indicating progressive vascular development during the 72 h observation period (Fig.4). However, substantial differences were observed among the samples. The uncoated Fe_3O_4 nanoparticles (A1) exhibited a gradual increase in vessel area from 19.0% at 0 h to 37.0% at 72 h. PEG-coated nanoparticles (A2) showed comparatively limited vascular expansion, increasing from 15.2% to 24.42% over the same period. In contrast, citric-acid-coated nanoparticles (A3) demonstrated a markedly enhanced angiogenic response, with vessel area increasing from 14.57% at 0 h to 47.86% at 72 h. A particularly notable increase was observed for A3 between 24 h and 48 h, where vessel area increased from 15.62% to 43.23%, indicating rapid vascular proliferation and neovascularization. The final vessel area recorded for A3 was approximately 1.3-fold higher than that of A1 and nearly two-fold higher than that of A2, demonstrating the pronounced influence of citric acid functionalization on vascular development.

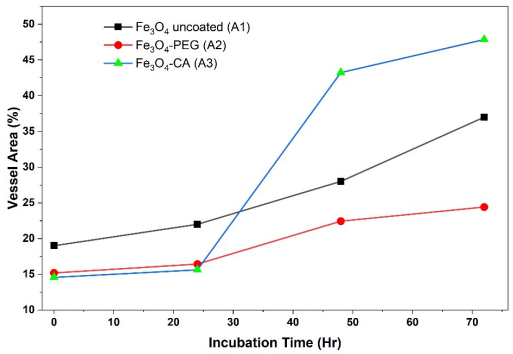

Fig. 4: Time-dependent changes in vessel area (%) of CAM treated with uncoated (A1), PEG-coated (A2), and citric-acid-coated (A3) Fe_3O_4 nanoparticles. Vessel area was quantified using Fiji/ImageJ image analysis as a measure of angiogenic response.

3.4.2 Branch Count Analysis

Vascular branching analysis further supported the angiogenic trends observed in the vessel area measurements (Fig.5). Branch formation reflects the complexity and maturation of the vascular network and is considered a reliable indicator of angiogenic progression. The branch count for A1 increased from 60 at 0 h to 173 at 72 h, indicating moderate vascular development. A2 exhibited a substantially greater increase, reaching 230 branches after 72 h. The highest branching density was observed for A3, where branch count increased from 74 at 0 h to 236 at 72 h. Moreover, A3 displayed the highest branch counts at every incubation interval, suggesting continuous stimulation of vascular growth throughout the experimental period. Although A1 showed an increase in branch count over time, the simultaneous occurrence of hemorrhage, vascular lysis, and coagulation observed during the HET-CAM assay suggests that these vascular changes may not exclusively represent healthy angiogenesis. In contrast, the extensive branching observed for A2 and A3 occurred in the absence of significant vascular damage, indicating favourable vascular compatibility and genuine angiogenic stimulation.

The quantitative image analysis strongly corroborates the qualitative HET-CAM observations and confirms that surface functionalization significantly influences nanoparticle-induced vascular responses. Among the investigated formulations, A3 exhibited the highest vessel area percentage and branch density, demonstrating the strongest angiogenic activity. A2 showed moderate angiogenic behaviour with excellent vascular compatibility, whereas A1 displayed comparatively lower angiogenic

performance and evidence of vascular irritation. Collectively, these findings indicate that citric acid functionalization provides the most favourable balance between vascular compatibility and angiogenic stimulation among the investigated Fe_3O_4 nanoparticle formulations.

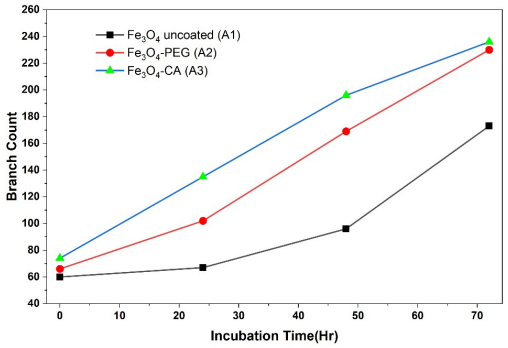

Fig. 5: Branch count of CAM vasculature following treatment with A1, A2, and A3 Fe_3O_4 nanoparticles over 72 h.

4. CONCLUSION

Surface functionalization significantly influenced the biological performance of Fe_3O_4 nanoparticles. The uncoated Fe_3O_4 nanoparticles (A1) exhibited the strongest antioxidant activity, whereas PEG-coated nanoparticles (A2) demonstrated superior membrane stabilization and hemocompatibility. Citric-acid-coated nanoparticles (A3) showed the most favourable angiogenic response, characterized by enhanced vessel area, increased branch formation, and excellent vascular compatibility in the HET-CAM model.

The results indicate that different surface coatings selectively optimize distinct biological properties of Fe_3O_4 nanoparticles. While exposure of the magnetic core favours free-radical scavenging, PEG functionalization improves blood compatibility and citric acid coating promotes vascular development. These findings highlight the critical role of surface engineering in tailoring nanoparticle-biological interactions and demonstrate that the biological performance of Fe_3O_4 nanoparticles is governed not only by the magnetic core but also by the nature of the surface modification.

Overall, surface-functionalized Fe_3O_4 nanoparticles represent promising candidates for future biomedical and drug-delivery applications. Further cell-based and in vivo investigations are warranted to validate their therapeutic potential and long-term biological safety.

ACKNOWLEDGEMENTS

The authors thank the Head and staff of the Department of Physics, University of Mumbai, for their timely support. The authors also acknowledge the UGC-DAE Consortium for Scientific Research (CSR), Mumbai Centre, for providing magnetization measurement facilities and thank the Director and faculty members for their assistance. The support of the Director and Deans, A.I Kalsekar Technical Campus (AIKTC), New Panvel, is also gratefully acknowledged. The authors further acknowledge the instrumentation facilities provided by SAIF, IIT Bombay, and CFC-SAIF, Shivaji University, Kolhapur, accessed through the iSTEM facility, for characterization support and infinite biotech laboratory, Sangli for bioactivities studies.

REFERENCES

1. Gupta AK, Gupta M. Synthesis and surface engineering of iron oxide nanoparticles for biomedical applications. biomaterials. 2005 Jun 1;26(18):3995-4021.
2. Laurent S, Forge D, Port M, Roch A, Robic C, Vander Elst L, Muller RN. Magnetic iron oxide nanoparticles: synthesis, stabilization, vectorization, physicochemical characterizations, and biological applications. Chemical reviews. 2008 Jun 11;108(6):2064-110.
3. Pankhurst QA, Connolly J, Jones SK, Dobson JJ. Applications of magnetic nanoparticles in biomedicine. Journal of physics D: Applied physics. 2003 Jul 7;36(13):R167-81.
4. Wahajuddin N, Arora S. Superparamagnetic iron oxide nanoparticles: magnetic nanoplatforms as drug carriers. International journal of nanomedicine. 2012 Jul 6:3445-71.
5. Sun C, Lee JS, Zhang M. Magnetic nanoparticles in MR imaging and drug delivery. Advanced drug delivery reviews. 2008 Aug 17;60(11):1252-65.
6. Lu AH, Salabas EE, Schüth F. Magnetic nanoparticles: synthesis, protection, functionalization, and application. Angewandte chemie international edition. 2007 Feb 12;46(8):1222-44.
7. Laurent S, Mahmoudi M. Superparamagnetic iron oxide nanoparticles: promises for diagnosis and treatment of cancer. International journal of molecular epidemiology and genetics. 2011 Nov 25;2(4):367.
8. Ling D, Hyeon T. Chemical design of biocompatible iron oxide nanoparticles for medical applications. Small. 2013 May 27;9(9-10):1450-66.
9. Sanità G, Carrese B, Lamberti A. Nanoparticle surface functionalization:

how to improve biocompatibility and cellular internalization. Frontiers in molecular biosciences. 2020 Nov 26;7:587012.
10. Jokerst JV, Lobovkina T, Zare RN, Gambhir SS. Nanoparticle PEGylation for imaging and therapy. Nanomedicine. 2011 Jun 1;6(4):715-28.
11. Owens III DE, Peppas NA. Opsonization, biodistribution, and pharmacokinetics of polymeric nanoparticles. International journal of pharmaceutics. 2006 Jan 3;307(1):93-102.
12. Bee A, Massart R, Neveu S. Synthesis of very fine maghemite particles. Journal of Magnetism and Magnetic Materials. 1995 Aug 1;149(1-2):6-9.
13. Thanh NT, Maclean N, Mahiddine S. Mechanisms of nucleation and growth of nanoparticles in solution. Chemical reviews. 2014 Aug 13;114(15):7610-30.
14. Chowdhury A, Azam S, Jainul MA, Faruq KO, Islam A. Antibacterial activities and in vitro anti-inflammatory (membrane stability) properties of methanolic extracts of Gardenia coronaria leaves. International journal of microbiology. 2014;2014(1):410935.
15. Oyedapo OO, Famurewa AJ. Antiprotease and membrane stabilizing activities of extracts of Fagara zanthoxyloides, Olax subscorpioides and Tetrapleura tetraptera. International journal of Pharmacognosy. 1995 Jan 1;33(1):65-9.
16. Halliwell B, Gutteridge JM. Free radicals in biology and medicine. Oxford university press; 2015.
17. Brand-Williams W, Cuvelier ME, Berset CL. Use of a free radical method to evaluate antioxidant activity. LWT-Food science and Technology. 1995 Jan 1;28(1):25-30.
18. Baliyan S, Mukherjee R, Priyadarshini A, Vibhuti A, Gupta A, Pandey RP, Chang CM. Determination of antioxidants by DPPH radical scavenging activity and quantitative phytochemical analysis of Ficus religiosa. Molecules. 2022 Feb 16;27(4):1326.
19. Ribatti D. The chick embryo chorioallantoic membrane (CAM) assay. Reproductive toxicology. 2017 Jun 1;70:97-101.
20. Naik M, Brahma P, Dixit M. A cost-effective and efficient chick ex-ovo CAM assay protocol to assess angiogenesis. Methods and protocols. 2018 May 31;1(2):19.
21. Vargas A, Zeisser-Labouèbe M, Lange N, Gurny R, Delie F. The chick embryo and its chorioallantoic membrane (CAM) for the in vivo evaluation of drug delivery systems. Advanced drug delivery reviews. 2007 Sep 30;59(11):1162-76.
22. Mahmoudi M, Hofmann H, Rothen-Rutishauser B, Petri-Fink A. Assessing the in vitro and in vivo toxicity of superparamagnetic iron oxide nanoparticles. Chemical reviews. 2012 Apr 11;112(4):2323-38.
23. Shaikh Arif, Radha S (2026). Influence of Surface Functionalization on the Colloidal Stability and Magnetic Properties of Ferrite Nanoparticles. arXiv preprint. https://arxiv.org/abs/2601.06585.